Self-Propagating Patterns in Active Filament Bundles

K. Kruse,[1,2] S. Camalet,[1] and F. Jülicher[1]

[1]*Institut Curie, Physicochimie, UMR CNRS/IC 168, 26 rue d'Ulm, 75248 Paris Cedex 05, France*
[2]*Max-Planck-Institut für Strömungsforschung, Bunsenstrasse 10, D-37073 Göttingen, Germany*

(Received 15 December 2000; published 11 September 2001)

Bundles of polar filaments which interact via active elements can exhibit complex dynamic behaviors. By using a simple and general description for the bundle dynamics, we find regimes for which density profiles propagate as solitary waves with a characteristic velocity along the bundle. These behaviors emerge from an interplay of local contractions in the bundle and relative sliding of oppositely oriented filaments. By introducing filament binding to and detachment from a substrate, the system is able to generate net motion as a self-organization phenomenon.

DOI: 10.1103/PhysRevLett.87.138101 PACS numbers: 87.16.–b, 05.45.–a, 47.54.+r, 87.15.–v

Many eucariotic cells are motile and can crawl along solid substrates [1]. In these cells, the forces necessary for locomotion are generated by the cytoskeleton, a dynamic ensemble of proteins which consists mostly of actin filaments and microtubules. These filaments are elastic rodlike structures of polymerized actin and tubulin monomers, respectively. Various other cytoskeletal proteins control the filament lengths, their spatial organization, and their dynamics [2]. The mechanical forces generated by the cytoskeleton are mainly due to polymerization at filament tips and to the action of motor proteins such as myosins and kinesins, which are able to advance along filaments by transducing the chemical energy of ATP [2–4]. During cell locomotion, the actin cortex, which is the part of the cytoskeleton localized beneath the cell membrane, plays a key role. It has been found that fragments of fish epidermal keratocytes which lack the cell nucleus and the microtubule network are fully motile and may advance on a substrate [5]. Remarkably, under constant external conditions, these fragments exist in a nonmoving symmetric state as well as in a motile asymmetric state [6]. The nonmoving state is stable, but it can be transformed into the motile state by a sufficiently strong deformation of the cell fragment using micromanipulation techniques. This observation suggests that cell motility mediated by the actin cytoskeleton is a self-organization phenomenon which is not regulated by a central unit such as, e.g., the nucleus.

In order to characterize basic mechanisms which are involved in the dynamic reorganization of the cytoskeleton in a living cell, *in vitro* experiments have been performed where the behavior of filaments in the presence of small aggregates of molecular motors is studied [7–9]. Filaments have two structurally different ends, denoted "plus" and "minus" and are thus polar constructs. A motor protein always moves along a filament towards the same end. Hence, aggregates of motors can induce relative displacements of two filaments when they simultaneously interact with both. In the presence of a large number of motor aggregates and filaments, this gives rise to interesting self-organization phenomena. Notably, contraction of filament bundles [7] and the formation of asters [8] have been reported. The dynamic behavior of polar filaments which interact with motor aggregates has also been studied theoretically [10–12]. In particular, it was shown that filament bundles have the ability to contract and to generate tension by a generic physical mechanism [12].

Of particular interest is the question whether self-organization of motors and filaments alone can lead to filament patterns which propagate along the system and are accompanied by a net motion of filaments. In this Letter we show theoretically that active systems of interacting filaments can generate solitary waves, i.e., patterns of filament distributions which propagate with constant velocity along a filament bundle. The basic mechanism leading to propagating patterns can already be discussed within the framework of Ref. [12]. There, solitary waves result from an interplay of local contractions in the bundle induced by filaments of one orientation and the relative sliding of the two populations of oppositely oriented filaments. In order to obtain real locomotion as a self-organization phenomenon, we generalize our description and include the possibility of attachment and detachment of filaments to and from a substrate.

Consider a bundle of polar filaments, all aligned along the x axis. The bundle is characterized by the distributions of two filament populations: the densities $c^+(x)$ and $c^-(x)$ of filaments oriented with their plus end to the right and to the left, respectively. The time evolution of the densities of the two filament populations can be expressed as

$$\partial_t c^+ = D\partial_x^2 c^+ - \partial_x J^+, \tag{1}$$

$$\partial_t c^- = D\partial_x^2 c^- - \partial_x J^-, \tag{2}$$

where D is an effective diffusion coefficient. The active currents $J^\pm$ are generated by the action of molecular motors, which provide mobile cross-links between filaments in the bundle. In general, a given filament actively slides in a direction which is determined by its polarity and the polarity of the filaments with which it interacts. If we assume that two-filament interactions dominate, which is the

case for low motor densities or low motor processivity, the currents can be written as $J^{\pm} = J^{\pm\pm} + J^{\pm\mp}$, with

$$J^{\pm\pm}(x) = \alpha \int_0^{\ell} d\xi\, [c^{\pm}(x + \xi) - c^{\pm}(x - \xi)]c^{\pm}(x), \tag{3}$$

$$J^{\pm\mp}(x) = \mp\beta \int_{-\ell}^{\ell} d\xi\, c^{\mp}(x + \xi)c^{\pm}(x), \tag{4}$$

where the average velocities α and β characterize the interaction strength of parallel and antiparallel filaments, respectively. In the following we will use rather the dimensionless parameters $\bar{\alpha} \equiv \alpha\ell^2(c_0^+ + c_0^-)/D$ and $\bar{\beta} \equiv \beta\ell/D$, where $c_0^{\pm} = \frac{1}{L}\int_0^L dx\, c^{\pm}(x)$ are the average filament densities and L is the system size. The expressions given for the currents capture the symmetries of filament interactions. In particular, the dynamical Eqs. (1)–(4) conserve momentum, i.e., the integral over the total current $I = \int_0^L dx\, J$, with $J = J^{++} + J^{+-} + J^{-+} + J^{--}$, vanishes. Homogeneous filament distributions $c^{\pm}(x) = c_0^{\pm}$ are stationary states of the system. They are linearly stable for $\bar{\alpha} < \bar{\alpha}_c$, where $\bar{\alpha}_c \geq 0$ is a critical value. For $\bar{\beta} = 0$, the distributions c^+ and c^- are uncoupled. Depending on the parameters, a given initial distribution may in this case either relax to the homogeneous state or contract to a localized state.

For nonzero $\bar{\beta}$, the coupling of the two filament populations via (4) leads to oppositely directed filament currents which can give rise to oscillating and self-propagating filament patterns. Consider, for example, a system of size L with periodic boundary conditions (a contractile ring). For $\bar{\beta} \neq 0$ we find numerically, within an interval $\bar{\alpha}_d < \bar{\alpha} < \bar{\alpha}_c^!$, limit cycles for which both filament distributions are nonhomogeneous and propagate in the same direction with the same velocity. These self-propagating patterns are solitary waves which can be expressed as

$$c^{\pm}(x, t) = u^{\pm}(x - vt), \tag{5}$$

where $u^{\pm}(x)$ is a time-independent filament profile. Numerically obtained solitary waves consist of one well-localized distribution $u^{\pm}$ of filaments pointing in one direction, while the distribution of filaments of opposite orientation $u^{\mp}$ is comparatively broad (see Fig. 1). Both distributions $u^{\pm}$ have one maximum, with the maximum corresponding to the localized distribution moving in front. Solitary waves exist for both equal and unequal numbers of filaments of the two orientations. For the special case of an equal number of filaments pointing in each direction, i.e., $c_0^+ = c_0^-$, the solitary wave is a state of broken symmetry between plus and minus filaments. Consequently, two different solitary waves which move in opposite directions exist. This coexistence of two stable self-propagating solutions which move in opposite directions can also occur in the asymmetric case. In the inset of Fig. 1 the velocity v of the propagation of solitary waves is presented for two different values of $\bar{\alpha}$ as a function of $\bar{\beta}$. For small $\bar{\beta}$ the velocity depends linearly on $\bar{\beta}$. For large $\bar{\beta}$ the velocity

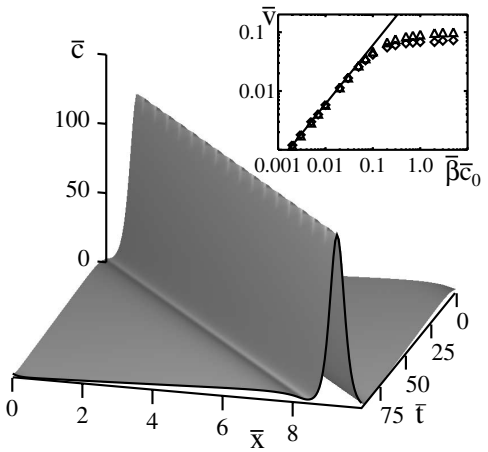

FIG. 1. Time evolution of the total density of filaments $\bar{c} = (c^+ + c^-)\ell$ for $\bar{\alpha} = 2$ and $\bar{\beta} = 0.1$ as a function of $\bar{x} = x/\ell$ and $\bar{t} = tD/\ell^2$ (numerical solution with spatial resolution $\Delta\bar{x} = 0.05$ and temporal resolution $\Delta\bar{t} = 6.25 \times 10^{-4}$). The system is of size $L = 10\ell$ with periodic boundary conditions, $c_0^+\ell = 3$ and $c_0^-\ell = 7$. The distribution is moving with constant velocity to the right with most of the minus filaments at the leading edge. The inset shows the velocity $\bar{v} = v\ell/D$ of self-propagating solutions as a function of $\bar{\beta}\bar{c}_0$ with $\bar{c}_0 = (c_0^+ + c_0^-)\ell$ for $\bar{\alpha} = 1.2$ (triangles) and $\bar{\alpha} = 2$ (diamonds), and all other parameters as above. The solid line is given by $\bar{v} = 2\bar{\beta}\ell c_0^+$ as obtained by the perturbation analysis; see text. All propagating solutions have been obtained from the same initial conditions.

saturates at a value which depends on $\bar{\alpha}$. However, for $\bar{\beta} = 0$ the slope $\partial v/\partial\bar{\beta}$ is independent of $\bar{\alpha}$ and L. The propagation of a pattern implies the existence of a local current J. Note, however, that, because of momentum conservation of Eqs. (1)–(4), the integrated current I vanishes.

For $\bar{\beta} \ll 1$, solitary waves can be understood as emerging from a contracted distribution $u_0^-(x)$ that is stable at $\bar{\beta} = 0$ which is set in motion by interacting with the homogeneous distribution $u_0^+(x) = c_0^+$ which is also stable for $\bar{\beta} = 0$. The deformations of the filament distributions as well as the propagation velocity can be expanded in $\bar{\beta}$:

$$u^{\pm}(x) = u_0^{\pm}(x) + u_1^{\pm}(x)\bar{\beta} + u_2^{\pm}\bar{\beta}^2 + \ldots, \tag{6}$$

$$v = v_1\bar{\beta} + v_3\bar{\beta}^3 + \ldots. \tag{7}$$

Here, all even terms vanish by symmetry in the expansion of v. Indeed, if $u^{\pm}(x - vt)$ is a solution for a given value of β, then $u^{\pm}(-x + vt)$ corresponds to $-\beta$, thus $v(\beta) = -v(-\beta)$. We obtain a solitary wave solution by assuming that u_0^- is localized while $u_0^+ = c_0^+$ is homogeneous [13]. In first order in $\bar{\beta}$, the corrections to the filament densities are then given by $u_1^-(x) = 0$, $u_{1,0}^+ = 0$, and

$$u_{1,k}^+ = \frac{2Di\,\sin k\ell\, c_0^+\, u_{0,k}^-}{D\ell k^2 + 2\alpha\ell(\cos k\ell - 1)c_0^+}, \tag{8}$$

for $k = 2\pi n/L \neq 0$, where $u_1^+(x) = \sum_k u_{1,k}^+ e^{ikx}$ and $u_0^-(x) = \sum_k u_{0,k}^- e^{ikx}$. For the velocity we obtain $v_1 = 2Dc_0^+$, thus $v = 2\beta\ell c_0^+ + O(\beta^3)$. A comparison of this result to first order in $\bar{\beta}$ with a numerically obtained

solution is shown in Fig. 2 which displays the distributions $u^+(x)$ and $u^-(x)$ of plus and minus filaments of a solitary wave with an equal number of filaments of both orientations. Superimposed are the distributions $u_0^\pm + \bar{\beta} u_1^\pm$.

Solitary waves can be obtained via a dynamic instability from a state where the filament distributions of both orientations are homogeneous. This instability can be induced by increasing the value of $\bar{\alpha}$ for fixed $\bar{\beta}$. This is shown in Fig. 3 which displays the amplitude $|c_1^+| + |c_1^-|$ of the first spatial Fourier component $c_1^\pm(t) = \frac{1}{L}\int_0^L dx\, c^\pm(x,t) e^{2\pi i x/L}$ of the filament distributions as a function of $\bar{\alpha}$. The homogeneous state with $|c_1^+| + |c_1^-| = 0$ is linearly stable for $\bar{\alpha} < \bar{\alpha}_c$. Propagating solutions with time-independent $|c_1^+| + |c_1^-| \neq 0$ exist for $\bar{\alpha} > \bar{\alpha}_d$. The bifurcation at $\bar{\alpha} = \bar{\alpha}_c$ that leads to solitary waves is subcritical and both states coexist within the interval $\bar{\alpha}_d < \bar{\alpha} < \bar{\alpha}_c$ [14]. If $\bar{\alpha}$ is increased further, a subsequent bifurcation occurs at which the solitary wave becomes unstable with respect to a second frequency. In Fig. 3 this type of solution is represented by triangles. We can estimate the propagation velocity expected in a bundle of actin filaments. The parameters chosen for Fig. 1 correspond, e.g., to the values $\alpha = 0.1\ \mu\mathrm{m\,s^{-1}}$, $\beta = 1\ \mu\mathrm{m\,s^{-1}}$, $D = 0.5\ \mu\mathrm{m^2\,s^{-1}}$, $\ell = 1\ \mu\mathrm{m}$, $c_0^+ = 3\ \mu\mathrm{m^{-1}}$, and $c_0^- = 7\ \mu\mathrm{m^{-1}}$. For these parameters the system self-organizes into a solitary wave with $v \approx 0.05\ \mu\mathrm{m\,s^{-1}}$.

The solitary waves discussed so far represent the most simple example for traveling patterns in actively interacting filament systems. Because of momentum conservation in this system, there is, however, no net filament current generated. We can generalize our discription and allow for momentum exchange with a substrate by introducing filament adhesion. We denote attachment and detachment rates of filaments to the substrate by ω_a and ω_d, respectively, and introduce the densities $a^+(x)$ and $a^-(x)$ of adhering and thus immobile filaments of both orientations, which satisfy the equation

$$\partial_t a^\pm(x) = \omega_a c^\pm(x) - \omega_d a^\pm(x). \tag{9}$$

In the presence of adhering filaments, Eqs. (1) and (2) governing the dynamics of the free filament densities c^+ and c^- have to be modified:

$$\partial_t c^\pm = D\partial_x^2 c^\pm - \partial_x J^\pm - \partial_x J_{\mathrm{adh}}^\pm - \omega_a c^\pm + \omega_d a^\pm. \tag{10}$$

Equation (10) takes into account the currents induced by adhering filaments which are given by

$$J_{\mathrm{adh}}^{\pm\pm}(x) = \alpha \int_0^\ell d\xi\, [a^\pm(x+\xi) - a^\pm(x-\xi)] c^\pm(x), \tag{11}$$

$$J_{\mathrm{adh}}^{\pm\mp}(x) = \mp\beta \int_{-\ell}^{\ell} d\xi\, a^\mp(x+\xi) c^\pm(x). \tag{12}$$

These expressions are consistent with Eqs. (3) and (4). Also, in the system (9)–(12), the homogeneous state is unstable for $\alpha > \alpha_c'$, where the critical value α_c' is positive and depends on ω_a and ω_d.

For $\beta \neq 0$, this instability leads to solitary wave solutions which, as a result of adhesion, are accompanied by a nonvanishing net filament current $I = \int_0^L dx\, (J_{\mathrm{adh}}^+ + J_{\mathrm{adh}}^-)$, i.e., the system is self-propelling (see Fig. 4). Note that this net current is a direct consequence of the solitary

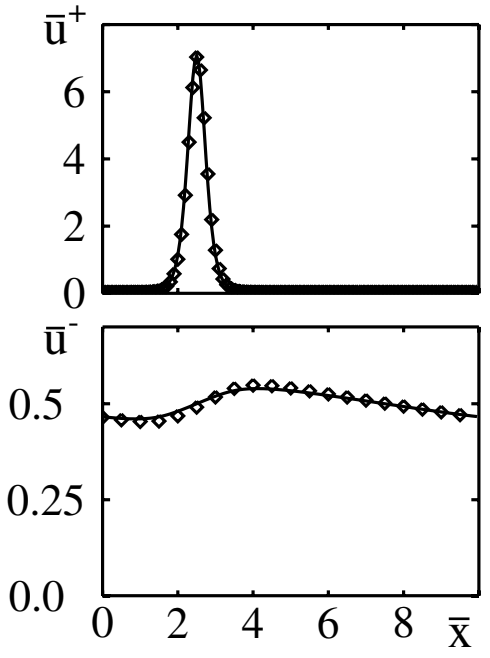

FIG. 2. Comparison of a numerically obtained solitary wave with the results of the perturbation calculation. The diamonds represent the distributions $\bar{u}^+ = u^+\ell$ of plus (upper frame) and $\bar{u}^- = u^-\ell$ of minus filaments (lower frame) of a solitary wave moving to the left for $\bar{\alpha} = 1.7$, $\bar{\beta} = 0.001$, $c_0^\pm \ell = 5$. The solid lines show the perturbative solution in first order in $\bar{\beta}$.

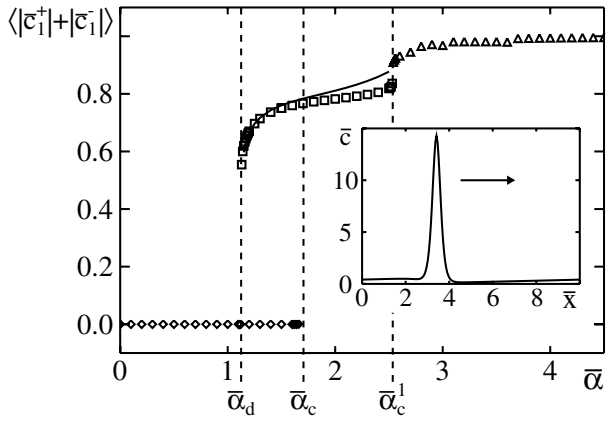

FIG. 3. The time averaged sum of the amplitudes of the first spatial Fourier components $\bar{c}_1^\pm = c_1^\pm \ell$ of the filament distributions as a function of $\bar{\alpha}$ for $\bar{\beta} = 0.01$ and all other parameters as in Fig. 1. The homogeneous solution is represented by diamonds, solitary waves by squares, and propagating oscillatory solutions by triangles. The solid line represents the solitary waves obtained by the perturbation calculation in first order in $\bar{\beta}$. The inset shows the distribution of the solitary wave for $\bar{\alpha} = 1.5$ moving in the direction indicated by the arrow.

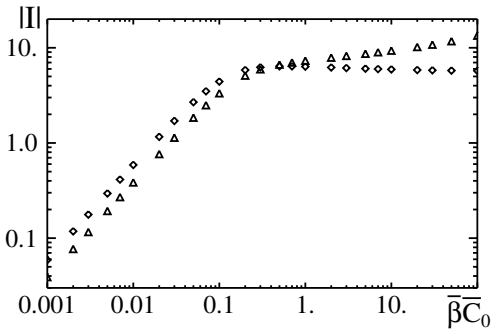

FIG. 4. The absolute value of the integrated filament current $|I|$ due to adhering filaments as a function of $\bar{\beta}\bar{C}_0$ for $\omega_a = 0.2$, $\omega_d = 1$, $(c_0^+ + a_0^+)/(c_0^- + a_0^-) = 3/7$, $\bar{\alpha} = 1.2$ (triangles), and $\bar{\alpha} = 2$ (diamonds), and all other parameters as in Fig. 1. Here, $\bar{C}_0 = (c_0^+ + a_0^+ + c_0^- + a_0^-)/\ell$ is the total number of filaments. Note that the sign of I is opposite to the sign of the velocity v.

wave. It vanishes in the homogeneous state according to Eqs. (9)–(12).

A symmetric system is a particular situation with $c_0^+ = c_0^-$ which generates at the instability self-propelling states via spontaneous symmetry breaking. It is interesting to note that this is phenomenologically reminiscent of the behavior observed for fish epidermal keratocyte fragments which exist in a symmetric nonmoving state and are able to move after the symmetry is broken by external manipulation. Our analysis shows that this type of behavior and the appearance of propagating filament patterns in general could already be found in simpler systems. In particular, these phenomena could be studied *in vitro* in experiments on actin filaments and myosin motors that interact with a substrate or the lipid bilayer membrane of a vesicle. Furthermore, contractile rings provide examples of active filament bundles within cells whose geometry corresponds to periodic boundary conditions and which could thus exhibit the dynamic patterns discussed here.

In this Letter we have presented the most simple examples of filament systems that exhibit propagating patterns and filament motion via self-organization of filaments and active elements. These behaviors can be expected to be generic, since the dynamic equations from which they follow are based on general symmetry arguments, which are independent of the details of the microscopic mechanisms. Indeed, the dynamic patterns described above also occur in generalizations of our description [15]. For example, we have numerically found propagating patterns when also incorporating the dynamic evolution of the density of active elements. Even though our description is very simplified, we expect that the basic physical mechanisms described here play a fundamental role in the dynamic organization of the cytoskeleton in living cells and during cell locomotion.

We thank J. Prost for valuable discussions. K. K. acknowledges the kind hospitality of the Landau Institute for Theoretical Physics, Moscow, where part of the work was accomplished.

[1] D. Bray, *Cell Movements* (Garland Publishing, New York, 1992).
[2] T. Kreis and R. Vale, *Cytoskeletal and Motor Proteins* (Oxford University Press, New York, 1993).
[3] J. Howard, Nature (London) **389**, 561 (1997).
[4] F. Jülicher, A. Ajdari, and J. Prost, Rev. Mod. Phys. **69**, 1269 (1997).
[5] U. Euteneuer and M. Schliwa, Nature (London) **310**, 58 (1984).
[6] A. B. Verkhovsky, T. M. Svitkina, and G. G. Borisy, Curr. Biol. **9**, 11 (1999).
[7] K. Takiguchi, J. Biochem. **109**, 502 (1991).
[8] F. J. Nédélec *et al.,* Nature (London) **389**, 305 (1997).
[9] T. Surrey *et al.,* Proc. Natl. Acad. Sci. U.S.A. **95**, 4293 (1998).
[10] H. Nakazawa and K. Sekimoto, J. Phys. Soc. Jpn. **65**, 2404 (1996).
[11] K. Sekimoto and H. Nakazawa, in *Current Topics in Physics,* edited by Y. M. Cho, J. B. Hong, and C. N. Yang (World Scientific, Singapore, 1998), Vol. 1, p. 394; Report No. physics/0004044.
[12] K. Kruse and F. Jülicher, Phys. Rev. Lett. **85**, 1778 (2000).
[13] For $\beta = 0$ the homogeneous and localized distributions may coexist for filaments of a given orientation [12]. Therefore solitary waves can be obtained in this way even if the system contains an equal number of filaments of both orientations.
[14] Note that, for some system sizes L, the bifurcation at $\bar{\alpha} = \bar{\alpha}_c$ is supercritical. For small $\bar{\beta}$ this is true for $4/(4n - 1) < L/\ell < 4/(4n - 3)$, $n = 1, 2, \ldots$.
[15] K. Kruse and F. Jülicher (unpublished).